Shape Design of Pin-Jointed Multi-Stable Compliant Mechanisms Using Snapthrough Behavior[1]

M. Ohsaki

Department of Architecture and Architectural Engineering,
Kyoto University Kyotodaigaku-Katsura, Nishikyo, Kyoto 615-8540, Japan
E-mail: ohsaki@archi.kyoto-u.ac.jp

S. Nishiwaki

Department of Precision Engineering, Kyoto University, Sakyo, Kyoto 606-8501, Japan

Abstract
A general approach is presented for generating pin-jointed multi-stable compliant mechanisms utilizing snapthrough behavior. An optimization problem is formulated for minimizing the total structural volume under constraints on the displacements at the specified nodes, stiffnesses at initial and final states, and load factors to lead to snapthrough behavior. The design variables are cross-sectional areas and the nodal coordinates. It is shown in the numerical examples that several mechanisms can be naturally found as a result of optimization starting from randomly selected initial solutions. It is also shown that no local bifurcation point exists along the equilibrium path, and the obtained mechanism is not sensitive to initial imperfections.

Keywords Compliant mechanism; Multi-stable structure; Shape optimization; Imperfection sensitivity; Snapthrough

1 Introduction

A compliant mechanism that utilizes flexibility of mechanical structure to generate large deformation has been recently proposed and developed for practical applications (Howell, 2001; Larsen *et al.*, 1996; Masters and Howell, 2003). In compliant mechanism, contrary to conventional mechanism based on unstable bar-joint model, the desired mechanical property is realized by appropriately placing flexible units in the structure. However, in most of the studies on compliant mechanism, the effect of geometrical nonlinearity is not incorporated, and the external loads should be applied to keep the deformed shape.

A structure that has two stable self-equilibrium states is called *bistable structure* (Pellegrino, 2002). If the compliant mechanism can utilize the effect of buckling behaviors such as snapthrough and bifurcation to generate a bistable structure (Matoba *et al.*, 1994), no external load is needed to retain the deformed shape.

[1]This paper has appeared in: Struct. Multidisc. Optim., Vol. 30, pp. 327–334, 2005.

Optimization of shape and topology is divided into two approaches based on continuum formulation and discrete model. The well-developed method of topology optimization of continuum can be effectively used for generating compliant mechanisms. Sigmund (1997) used SIMP (Solid Isotropic Microstructure with Penalization) approach, and Nishiwaki *et al.* (2001) used homogenization method for generating mechanisms under assumption of small deformation. Pedersen *et al.* (2002) and Bruns and Tortorelli (2001) incorporated the effect of large deformation including snapthrough behavior in the optimization process. Their methods, however, do not obtain mechanisms to generate large deformation under small forces. Bruns *et al.* (2002) and Sekimoto and Noguchi (2001) presented methods utilizing the effect of snapthrough. However, no mechanism has been generated in their studies.

Recently, optimization considering geometrically nonlinear buckling has been extensively studied (Ohsaki and Nakamura, 1994; Ohsaki, 2000). Bruns and Sigmund (2004) presented an optimization method in continuum formulation for generating compliant mechanisms utilizing snapthrough behavior. Various difficulties have been overcome by introducing three-stage approach to restrict the design space. In this paper, a straightforward and explicit formulation is presented to naturally generate a mechanism that exhibits snapthrough behavior. A truss model is used to avoid difficulties such as checkerboard problem in continuum model.

One of the major difficulties of optimization considering geometrical nonlinearity is that there may exist many local buckling modes that lead to divergence in the analysis and optimization processes. Another difficulty exists in imperfection sensitivity of the optimal solution (Thompson, 1969). If a bifurcation point exists along the equilibrium path before reaching the final state, the equilibrium path may be quite different from that of the ideal structure due to inevitable manufacturing errors.

In this study, a new problem formulation is presented for shape optimization of compliant mechanism. The difficulties due to local instability are avoided by using bar-joint model rather than continuum approach. A single-step formulation is presented to generate a multi-stable mechanism that exhibits snapthrough. Several new types of mechanisms are obtained by optimizing the cross-sectional areas and nodal locations. No preprocessing is needed in the proposed method, and several mechanisms can be found by simply optimizing from randomly generated initial ground structures. It is shown in the numerical examples that the shape of the equilibrium path of the optimal solution is not sensitive to initial imperfection.

2 Multi-stable compliant mechanism

Consider a structure as shown in Fig. 1. A multi-stable compliant mechanism in this paper is defined as follows:

1. A large displacement $U_{\mathrm{A}r}$ is generated at point A in the rth specified direction as a result of forced displacement U_r at point r of the structure, where $r = 1, 2, \ldots, N^{\mathrm{p}}$ and N^{p} is the number of loading conditions.
2. The deformed states can be retained without applying external loads; i.e. the structure has $N^{\mathrm{p}} + 1$ self-equilibrium states including the undeformed initial state.

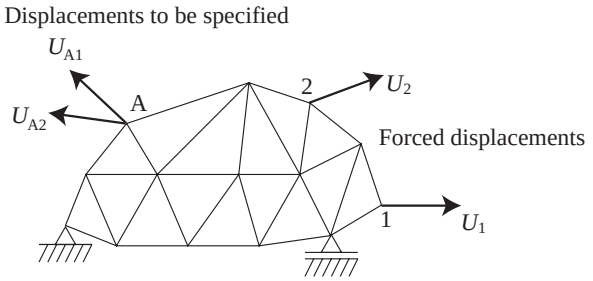

Fig. 1: Specified displacements U_{A1} and U_{A2}, respectively, by forced displacements U_1 and U_2.

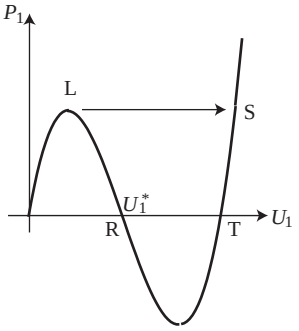

Fig. 2: Relation between force and displacement of a structure exhibiting limit-point-type instability.

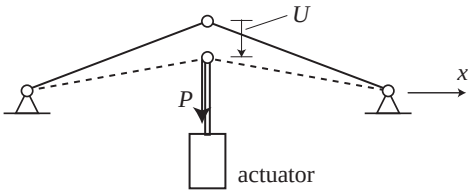

Fig. 3: A 2-bar truss.

3. The undeformed shape can be recovered by reversely applying small force as a disturbance at each deformed state.

The multi-stable structure can be realized by utilizing the snapthrough behavior, where the deformation is controlled by displacements with actuators. Fig. 2 illustrates the relation between the forced displacement U_1 and the reaction P_1 which is the force applied by the actuator. Consider a process of increasing U_1 by pulling an actuator from the undeformed initial state. P_1 increases until reaching the limit point L, and decreases if U_1 is further increased beyond the limit point. If the deformation is controlled by P_1, the equilibrium state jumps from L to S by a dynamic behavior called snapthrough.

Let U_1^* denote the value of U_1 at R in Fig. 2 satisfying $P_1 = 0$ beyond the limit point. Suppose the actuator is locked at R. Note that this equilibrium state is stable

because the actuator has extensional stiffness. This way, a bistable mechanism that has self-equilibrium states $U_1 = 0$ and $U_1 = U_1^*$ can be generated.

For example, consider a 2-bar truss as shown in Fig. 3, where the solid and dotted lines are the shapes before and after deformation, respectively. If the vertical displacement U of the center node is increased, P increases and reaches a limit point. By further increasing U, $P = 0$ is satisfied when the two bars are colinear in the horizontal position, and a self-equilibrium state can be retained by locking the actuator at this state without any extensional force. For general cases with multiple loading conditions, this process is extended to generate multi-stable structures by utilizing snapthrough.

Remark 1 *For the 2-bar truss, the state T corresponds to a stable self-equilibrium state that is reverse to the initial state with respect to the x-axis. Therefore it is possible that this stable state is used to generate a multi-stable structure without locking the actuator. However, we assign the condition such that the initial state should be recovered by small disturbance at the final state. Therefore we use point R rather than T in Fig. 2.*

3 Optimization problem

An optimization problem is formulated for a finite dimensional structure such as trusses. Although a plane structure is used in the following for simple presentation of the method, the proposed method can be naturally extended to three-dimensional cases.

The design requirements are summarized as

1. The deformation is controlled by displacements, and a large deformation is generated by utilizing snapthrough behavior.
2. The load at the final state for each loading condition is 0, and the final configuration can be retained by constraining the loaded degree of freedom.
3. The total structural volume is minimized.
4. The structure has enough initial stiffness.
5. The structure also has enough stiffness at each final state after constraining the loaded degree of freedom.
6. The initial state can be recovered by releasing the additional constraints and applying a small disturbance reversely at the final state.

The final state is defined such that the displacement $U_{\mathrm{A}r}$ in the rth specified direction of output node A reaches the specified large value $\bar{U}_{\mathrm{A}r}$ as a result of forced displacement at input node r. The values corresponding to the final state is denoted by the superscript f; i.e.

$$U_{\mathrm{A}r}^{\mathrm{f}} = \bar{U}_{\mathrm{A}r}^{\mathrm{f}}, \quad (i = 1, 2, \ldots, N^{\mathrm{p}}) \tag{1}$$

Note that the input displacements and forces are assumed to be positive for simple presentation of equations. The following constraint is given so that the final state is retained by applying a small additional constraining force by locking the actuator:

$$P_r^{\mathrm{f}} \leq 0, \quad (r = 1, 2, \ldots, N^{\mathrm{p}}) \tag{2}$$

where the constraint $P^{\mathrm{f}}_{\mathrm{A}r} = 0$ has been relaxed to inequality in (2) to improve convergence property in optimization process.

The displacement of node r at the final state is denoted by U^{f}_r. An upper bound $\bar{U}^{\mathrm{f}}_r$ is given for U^{f}_r as follows, instead of incorporating U^{f}_r in the objective function:

$$U^{\mathrm{f}}_r \leq \bar{U}^{\mathrm{f}}_r \tag{3}$$

Remark 2 *In the formulation of the optimization problem of compliant mechanism, the ratio of the absolute value of the output displacement $U^{\mathrm{f}}_{\mathrm{A}r}$ to the input displacement U^{f}_r is usually maximized. However, in this study, we have more than two loading conditions, and the total structural volume is to be minimized to generate a mechanism with small number of members. Hence, the final state is defined by the output displacement, and the input displacement is included in the constraints.*

Let U^0_r denote the linearly estimated displacement U_r for $P_r = 1$ at the initial state. The constraint on the initial stiffness is given as

$$U^0_r \leq \bar{U}^0_r, \quad (r = 1, 2, \ldots, N^{\mathrm{p}}) \tag{4}$$

where $\bar{U}^0_r$ is the specified upper bound. Let $U^{\mathrm{f0}}_{\mathrm{A}rx}$ and $U^{\mathrm{f0}}_{\mathrm{A}ry}$ denote the displacement in x- and y-directions of node A at the final state, respectively, for the unit loads in x- and y-directions at node A after constraining node r in the direction of U_r for rth loading condition. The constraints for the stiffness at the final state are assigned as

$$U^{\mathrm{f0}}_{\mathrm{A}rx} \leq \bar{U}^{\mathrm{f0}}_{\mathrm{A}x}, \quad U^{\mathrm{f0}}_{\mathrm{A}ry} \leq \bar{U}^{\mathrm{f0}}_{\mathrm{A}y}, \quad (r = 1, 2, \ldots, N^{\mathrm{p}}) \tag{5}$$

where $\bar{U}^{\mathrm{f0}}_{\mathrm{A}x}$ and $\bar{U}^{\mathrm{f0}}_{\mathrm{A}y}$ are the prescribed values, and the tangent stiffness is used for evaluating $U^{\mathrm{f0}}_{\mathrm{A}rx}$ and $U^{\mathrm{f0}}_{\mathrm{A}ry}$. Note that the constraints on stiffness together with that of the final load (2) lead to a solution that exhibits snapthrough behavior.

Let P^{m}_r denote the load at the intermediate state where $U_{\mathrm{A}r}$ reaches $\bar{U}_{\mathrm{A}r}/2$. To further improve convergence to a structure with limit point, the following constraint is given:

$$P^{\mathrm{m}}_r \geq P^{\mathrm{f}}_r \tag{6}$$

Bruns and Sigmund (2004) assigned constraints such that the displacement under higher load level should be sufficiently large, while the displacement at the initial small load level should be small. This way, a structure with decreasing stiffness can be found. However, large deformation at a higher load level does not assure existence of a limit point or bistable optimal solution.

The design variables are the cross-sectional areas $\mathbf{A} = \{A_j\}$ and nodal coordinates $\mathbf{X} = \{X_k\}$, where a subscript is used for indicating the component of a vector. A conventional ground structure approach is used, and the members with small cross-sectional areas are removed at the optimal solution. The optimization problem for

minimizing the total structural volume $V(\mathbf{A}, \mathbf{X})$ is stated as

$$
\begin{aligned}
\text{minimize} \quad & V(\mathbf{A}, \mathbf{X}) && (7)\\
\text{subject to} \quad & P_r^{\mathrm{f}}(\mathbf{A}, \mathbf{X}) \le 0, \quad (r = 1, 2, \ldots, N^{\mathrm{p}}) && (8)\\
& U_r^{\mathrm{f}}(\mathbf{A}, \mathbf{X}) \le \bar{U}_r^{\mathrm{f}}, \quad (r = 1, 2, \ldots, N^{\mathrm{p}}) && (9)\\
& U_r^{0}(\mathbf{A}, \mathbf{X}) \le \bar{U}_r^{0} \quad (r = 1, 2, \ldots, N^{\mathrm{p}}) && (10)\\
& U_{\mathrm{A}rx}^{\mathrm{f0}}(\mathbf{A}, \mathbf{X}) \le \bar{U}_{\mathrm{A}x}^{\mathrm{f0}}, \quad (r = 1, 2, \ldots, N^{\mathrm{p}}) && (11)\\
& U_{\mathrm{A}ry}^{\mathrm{f0}}(\mathbf{A}, \mathbf{X}) \le \bar{U}_{\mathrm{A}y}^{\mathrm{f0}}, \quad (r = 1, 2, \ldots, N^{\mathrm{p}}) && (12)\\
& P_r^{\mathrm{m}}(\mathbf{A}, \mathbf{X}) \ge P_r^{\mathrm{f}}, \quad (r = 1, 2, \ldots, N^{\mathrm{p}}) && (13)\\
& \mathbf{A}^{\mathrm{L}} \le \mathbf{A} && (14)\\
& \mathbf{X}^{\mathrm{L}} \le \mathbf{X} \le \mathbf{X}^{\mathrm{U}} && (15)
\end{aligned}
$$

where $\mathbf{X}^{\mathrm{U}}$ and $\mathbf{X}^{\mathrm{L}}$ are the upper an lower bounds for $\mathbf{X}$, and $\mathbf{A}^{\mathrm{L}} = \{A_j^{\mathrm{L}}\}$ consist of very small lower bound for $\mathbf{A}$ for preventing numerical instability. The member with $A_j = A_j^{\mathrm{L}}$ after optimization is to be removed.

Remark 3 *When the final value $\bar{U}_{\mathrm{A}r}^{\mathrm{f}}$ of the output displacement at node A and the upper bound $\bar{U}_r^{\mathrm{f}}$ of the input displacement are given, all the parameters in the problem can be defined without any trial-and-error process. Suppose that the upper-bound displacements $\bar{U}_r^0$, $\bar{U}_{\mathrm{A}x}^{\mathrm{f0}}$ and $\bar{U}_{\mathrm{A}y}^{\mathrm{f0}}$ for stiffness constraints are scaled by same factor α. Without changing the optimal nodal locations, the optimal solutions are scaled as*

$$
\begin{aligned}
& P_r^{\mathrm{f}} \to P_r^{\mathrm{f}}/\alpha, \quad U_r^{\mathrm{f}} \to U_r^{\mathrm{f}}, \quad U_r^0 \to \alpha U_r^0,\\
& U_{\mathrm{A}rx}^{\mathrm{f0}} \to \alpha U_{\mathrm{A}rx}^{\mathrm{f0}}, \quad U_{\mathrm{A}ry}^{\mathrm{f0}} \to \alpha U_{\mathrm{A}ry}^{\mathrm{f0}}, \quad P_r^{\mathrm{m}} \to P_r^{\mathrm{m}}/\alpha,\\
& \mathbf{A} \to \mathbf{A}/\alpha, \quad V \to V/\alpha
\end{aligned}
\qquad (16)
$$

Therefore, the total structural volume can be controlled by the parameter α after obtaining an optimal solution.

Obviously, the final state cannot be found if the direction of $U_{\mathrm{A}r}$ at the initial solution is opposite to $\bar{U}_{\mathrm{A}r}$. Furthermore, nonlinearities of both analysis and optimization problems to be solved in this study are very strong. Therefore, initial solutions are randomly generated, and several local optima are found to generate various types of compliant mechanisms. The optimization algorithm is summarized as follows:

Step 1 Randomly assign initial values of $\mathbf{A}$ and $\mathbf{X}$.

Step 2 Trace the equilibrium path for each loading condition by considering the displacement of node r as the path parameter.

Step 3 Go to Step 1 if $U_{\mathrm{A}r}$ at the first incremental step is opposite to $\bar{U}_{\mathrm{A}r}$. Otherwise, trace the path until (1) is satisfied.

Step 4 Compute sensitivity coefficients of the objective and constraint functions with respect to $\mathbf{A}$ and $\mathbf{X}$.

Step 5 Update $\mathbf{A}$ and $\mathbf{X}$ in accordance with an optimization algorithm.

Step 6 Go to Step 2 if not converged.

Step 7 Go to Step 1 if another mechanism is needed.

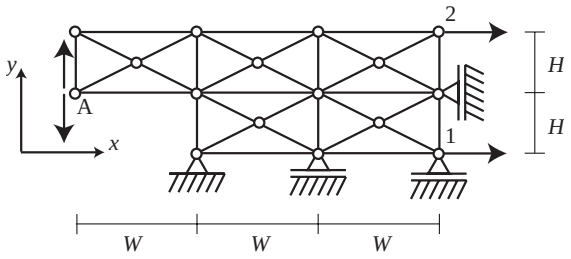

Fig. 4: A 35-bar plane truss model-1.

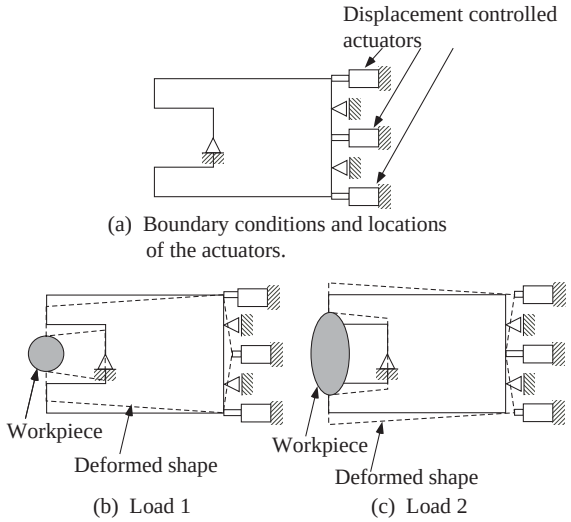

Fig. 5: Illustration of the mechanism.

4 Examples

Consider a 35-bar plane truss as shown in Fig. 4, which represents one of two equal parts that are symmetric with respect to x-axis, where $W = 0.2\,\mathrm{m}$, $H = 0.1\,\mathrm{m}$.

Two loading conditions are considered; i.e. a tri-stable mechanism is to be generated. A forced displacement U_1 and U_2 are given, respectively, in x-direction at nodes 1 and 2, and the final state is defined such that the displacements in y-direction of node A for loading conditions 1 and 2 reach the specified values $\bar{U}^{\mathrm{f}}_{\mathrm{A}1} = -0.02\,\mathrm{m}$ and $\bar{U}^{\mathrm{f}}_{\mathrm{A}2} = 0.02$ m, respectively. Other parameters are $\bar{U}^{\mathrm{f}}_r = \bar{U}^0_r = \bar{U}^{\mathrm{f0}}_{\mathrm{A}x} = \bar{U}^{\mathrm{f0}}_{\mathrm{A}y} = 0.02\,\mathrm{m}$, where the unit of force is kN; i.e. the loads for computing U^0_r, $U^{\mathrm{f0}}_{\mathrm{A}x}$ and $U^{\mathrm{f0}}_{\mathrm{A}y}$ are 1 kN.

The truss represents a half of an equipment shown in Fig. 5(a), which illustrates the usage of the mechanism. If the size of the workpiece is larger than the initial gap as shown in Fig. 5(c), the node 2 is pulled to open the gap, stop at the final position, insert the workpiece, and release the actuator to close the gap. If the size of the workpiece is a little smaller than the initial gap as shown in Fig. 5(b), pull the actuator at node 1, release it slightly beyond the final state to grip the workpiece without external loads.

The cross-sectional areas of all members are independent variables with lower bound 1.0×10^{-6} m^2. The coordinates of node A and the supports in the constrained directions are fixed during optimization. Let x_i^0 denote the x-coordinate of an unconstrained node in the grid shown in Fig. 4. The upper and lower bounds of x_i are given by $x_i^0 \pm 0.02$ m. The feasible regions of the y-coordinates are defined similarly.

The rotated engineering strain is used; i.e. the member length after deformation is computed from the distance between the nodes connected by the member. The elastic modulus is 2.0×10^6 kN/m^2. The displacement increment method is used for tracing the equilibrium path, where U_r is taken as parameter with increment 2.0×10^{-4} m. The unbalanced loads are canceled at the subsequent step. To prevent divergence due to singularity of the tangent stiffness matrix, the effect of initial stress is not incorporated for predicting the responses after incremental step. However, the effect of changes of nodal locations are incorporated in the linear stiffness, and the unbalanced loads are confirmed to be sufficiently small. The accuracy of equilibrium analysis has also been confirmed by ANSYS Ver. 7.0.

Optimization is carried out by IDESIGN Ver. 3.5 (Arora and Tseng, 1987), where the sequential quadratic programming is used. The sensitivity coefficients are computed by the forward finite difference method. Computation is carried out on a PC with Xeon 2.80 GHz and 1 GB memory. Note that the purpose of this paper is to present a problem formulation and an algorithm that can generate various types of multi-stable mechanisms. However, the CPU time will be shown in each example to confirm that the optimal solutions are found within reasonable computational cost. The well-developed methods of analytical design sensitivity analysis can be used if computational cost should be reduced (Ohsaki, 2005).

A uniform random value $R_i \in [0, 1)$ is generated consecutively, and the initial value of A_i (m^2) is given as

$$A_i = 0.001 + 0.002(R_i - 0.5) \tag{17}$$

For the unconstrained nodal locations, the initial value of x_i (m) is given as

$$x_i = x_i^0 + 0.5(R_i - 0.5) \tag{18}$$

The y-coordinates are defined similarly.

Starting from different initial solutions, two local optimal solutions have been found. Type-1 solution is as shown in Fig. 6(a), where the width of each member is proportional to its cross-sectional area, and the thin members after optimization have been removed. The total structural volume is 1.3479×10^{-2} m^3, and the CPU time is 269 sec. The number of steps for optimization is 57. The final deformed shape for the loads at nodes 1 and 2, which are denoted by loads 1 and 2 for brevity, are as shown in Figs. 6(b) and (c), respectively.

The relation between U_1 and P_1 of Type-1 solution is plotted in the solid curve in Fig. 7. It is seen from Fig. 7 that P_1 increases as U_1 is increased before reaching a limit point. P_1 decreases by further increasing U_1 to reach the final state with $P_1 = 0$. Similar relation between P_2 and U_2 is plotted in solid curve in Fig. 8. It can be

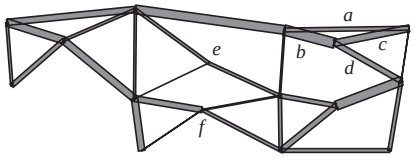

(a) Undeformed initial shape.

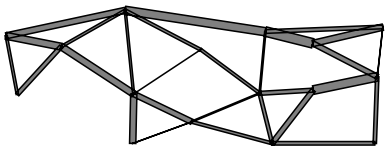

(b) Final shape for load 1

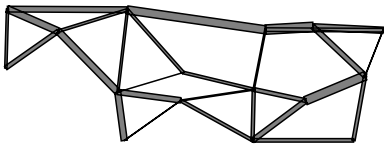

(b) Final shape for load 2

Fig. 6: Optimum design Type-1 ($V = 1.3479 \times 10^{-2}\,\mathrm{m}^3$).

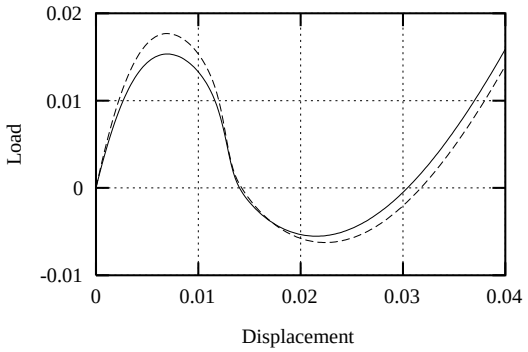

Fig. 7: Relation between U_1 and P_1 of the optimum design Type-1; solid curve: perfect structure; dashed curve: imperfect structure.

observed from Figs. 6(a) and (c) that snapthrough behavior takes place for load 2 at the triangular unit formed by members a, b and c. Let N_d denote the axial force of member d. The relation between U_2 and N_d is as shown in Fig. 9, which indicates existence of a limit point around $U_2 \simeq 0.007$. Local buckling is also observed around the nodes e and f for load 1.

It is well known that the equilibrium path may be drastically deviated due to initial imperfection if there is a bifurcation point along the equilibrium path. However, the bifurcation points cannot be detected from the shape of equilibrium path. To investigate imperfection sensitivity of the optimal solution, eigenvalue analysis is carried out at each incremental step for the tangent stiffness matrix incorporating the effect of initial stress without fixing the loaded degree of freedom. Fig. 10 shows the relation

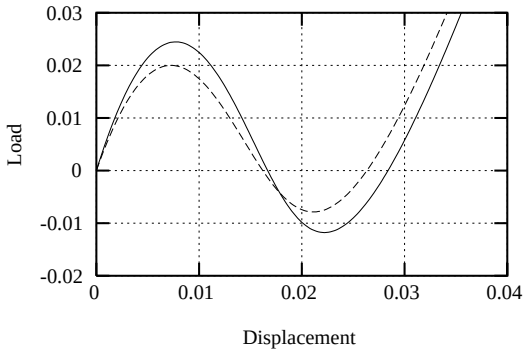

Fig. 8: Relation between U_2 and P_2 of the optimum design Type-1; solid curve: perfect structure; dashed curve: imperfect structure.

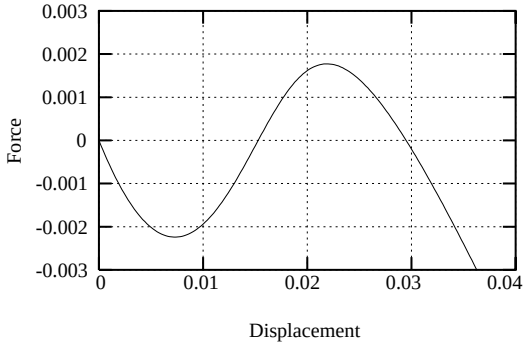

Fig. 9: Relation between U_2 and N_d of the optimum design Type-1.

between U_1 and the lowest two eigenvalues. It is confirmed from Fig. 7 and 10 that the lowest eigenvalue reaches 0 at the limit point. The second eigenvalue is positive until reaching the final state; i.e. there is no bifurcation point along the equilibrium path. The eigenvalues for load 2 are also plotted in Fig. 11, where similar properties as load 1 are observed.

To further investigate imperfection sensitivity, a uniform random value $R_i \in [0, 1)$

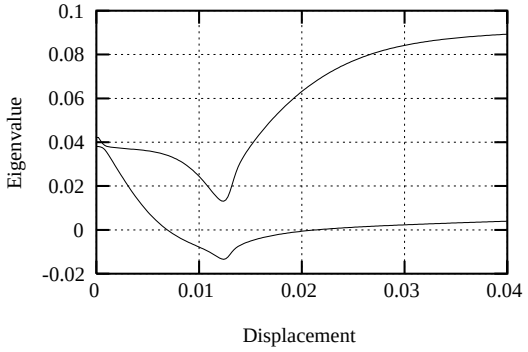

Fig. 10: Relation between U_1 and eigenvalues of the optimum design Type-1.

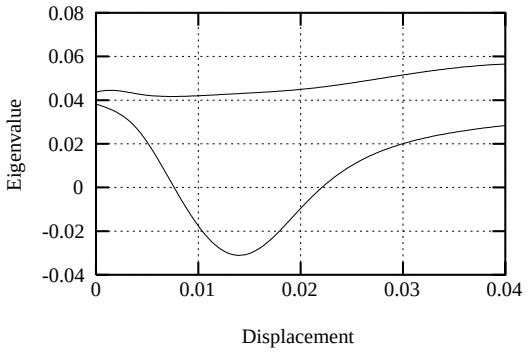

Fig. 11: Relation between U_2 and eigenvalues of the optimum design Type-1.

is generated to define the nodal locations of imperfect structures as

$$x_i = x_i^{\rm opt} + 0.002(R_i - 0.5) \tag{19}$$

where $x_i^{\rm opt}$ are the x-coordinates of the optimal solution in Fig. 6(a). y-coordinates are defied similarly.

Equilibrium paths have been traced for 10 cases of imperfect structures. Let D_i for the ith imperfect structure denote the mean absolute value of deviation of the load from that of the perfect structure throughout the incremental step before reaching the final state. The maximum value of D_i among the 10 cases for loads 1 and 2 are 1.4779×10^{-3} and 3.4687×10^{-3}, respectively, and the equilibrium paths corresponding to these worst cases are plotted in dashed curves in Figs. 7 and 8. It is seen from these results that the optimal solution is not sensitive to initial imperfections.

The Type-2 solution from a different initial solution is shown in Fig. 12, where the objective value is $1.8278 \times 10^{-2}\,\mathrm{m}^3$. The CPU time is 133 sec, and the number of steps for optimization is 28. Since Type-1 has the smaller objective value than Type-2, Type-1 is optimal in view of total structural volume. However, our objective is to generate various mechanisms from randomly generated initial structures.

Consider next a similar ground structure as shown in Fig. 13 with different boundary conditions and input displacements. The forced displacements are applied in the negative y-direction at nodes 3 and 4, respectively, to generate vertical displacements at node A, where $\bar{U}^{\rm f}_{\rm A3} = -0.02\,\mathrm{m}$ and $\bar{U}^{\rm f}_{\rm A4} = 0.02\,\mathrm{m}$. Other parameters are same as those in the previous examples.

The obtained Type-3 mechanism is shown in Fig. 14, where $V = 1.2683 \times 10^{-2}$ m^3. The CPU time is 153 sec, and the number of steps for optimization is 36. The relations between the loads and displacements for loads 3 and 4 of Type-3 mechanism are plotted in Figs. 15 and 16, respectively. It is seen from Fig. 14(b) that snapthrough behaviors are observed in the units (g, h, i) and (j, k, l) for loads 3 and 4, respectively.

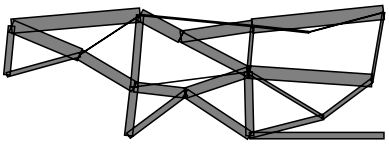

(a) Undeformed initial shape.

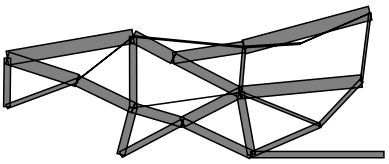

(b) Final shape for load 1

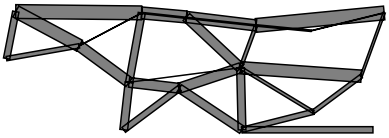

(c) Final shape for load 2

Fig. 12: Optimum design Type-2 ($V = 1.8278 \times 10^{-2}$ m^3).

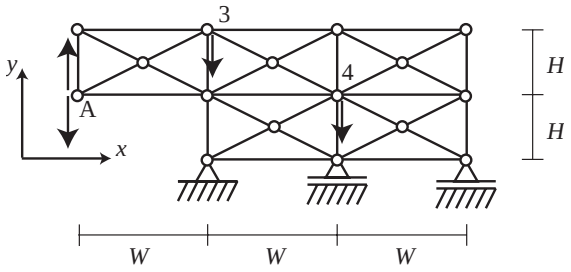

Fig. 13: A 35-bar plane truss model-2.

5 Conclusions

A new formulation is presented for generating multi-stable compliant mechanisms consisting of bar elements. The conclusions drawn from this study are summarized as follows:

1. A multi-stable structure that has more than two self-equilibrium states can be found by ground structure approach considering geometrical nonlinearity. The final state is defined such that the output displacement reaches the specified value, and the input displacement as well as the stiffness at the initial and final states are included in the constraints. This way, multi-stable mechanisms with small number of members can be successfully found by minimizing the total structural volume. More difficulties should be overcome if the proposed approach is to be extended to continuum models.
2. Various types of mechanisms can be found by optimizing from randomly generated initial solutions; i.e. the proposed method does not require multi-stage procedures

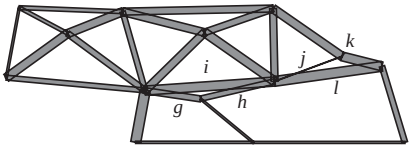

(a) Undeformed initial shape.

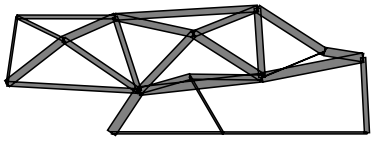

(b) Final shape for load 3

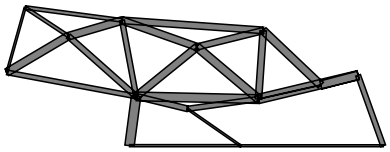

(c) Final shape for load 4

Fig. 14: Optimum design Type-3 ($V = 1.2683 \times 10^{-2}$ m^3).

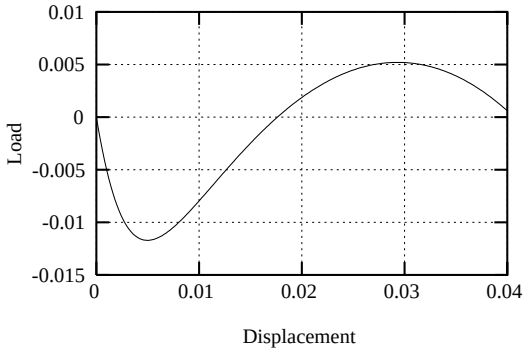

Fig. 15: Relation between U_3 and P_3 of the optimum design Type-3.

that involve human judgment. The difficulties in continuum formulations can be avoided by using bar elements.

3. The multi-stable mechanism with large deformation can be realized by local snapthrough behavior. Therefore, it may be possible that the number of members irrelevant to snapthrough are reduced without modifying the local units corresponding to snapthrough.

References

Arora, J. and Tseng, C. (1987). Idesign user's manual, ver. 3.5. Technical report, Optimal Design Laboratory, The University of Iowa.

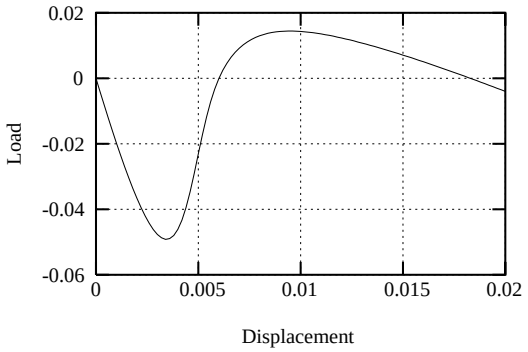

Fig. 16: Relation between U_4 and P_4 of the optimum design Type-3.

Bruns, T. E. and Sigmund, O. (2004). Toward the topology design of mechanisms that exhibit snap-through behavior. *Comp. Meth. Appl. Mech. Engng.*, **193**, 3973–4000.

Bruns, T. E. and Tortorelli, D. A. (2001). Topology optimization of non-linear structures and compliant mechanisms. *Comp. Meth. Appl. Mech. Engng.*, **190**, 3443–3459.

Bruns, T. E., Sigmund, O., and Tortorelli, D. A. (2002). Numerical methods for the topology optimization of structures that exhibit snap-through. *Int. J. Num. Meth. Engng.*, **55**, 1215–1237.

Howell, L. L. (2001). *Compliant Mechanisms*. John Wiley & Sons.

Larsen, U. D., Sigmund, O., and Bouswstra, S. (1996). Design and fabrication of compliant micromechanisms and structures with negative poisson's ratio. In *Proc. IEEE 9th Annual Int. Workshop on Micro Electro Mech. Sys., An Investigation of Micro Structures, Sensors, Actuators, Machines and Systems*, pages 365–371, San Diego, California.

Masters, N. D. and Howell, L. L. (2003). A self-retracting fully compliant bistable micromechanism. *J. MEMS*, **12**, 273–280.

Matoba, H., Ishikawa, T., Kim, C., and Muller, R. S. (1994). A bistable snapping mechanisms. *IEEE Micro Electoro Mech. Sys.*, **??**, 45–50.

Nishiwaki, S., Min, S., Yoo, J., and Kikuchi, N. (2001). Optimal structural design considering flexibility. *Comp. Meth. Appl. Mech. Engng.*, **190**, 4457–4504.

Ohsaki, M. (2000). Optimization of geometrically nonlinear symmetric systems with coincident critical points. *Int. J. Num. Meth. Engng.*, **48**, 1345–1357.

Ohsaki, M. (2005). Design sensitivity analysis and optimization for nonlinear buckling of finite-dimensional elastic conservative structures. *Compu. Meth. Appl. Mech. Engng.*, in press.

Ohsaki, M. and Nakamura, T. (1994). Optimum design with imperfection sensitivity coefficients for limit point loads. *Structural Optimization*, **8**, 131–137.

Pedersen, C. B. W., Buhl, T., and Sigmund, O. (2002). Topology optimization of large-displacement compliant mechanisms. *Int. J. Num. Meth. Engng.*, **44**, 1215–1237.

Pellegrino, S. (2002). *Deployable Structures*. Springer.
Sekimoto, T. and Noguchi, H. (2001). Homologous topology optimization in large displacement and buckling problems. *JSME Int. J., Series A*, **44**, 610–615.
Sigmund, O. (1997). On the design of compliant mechanisms using topology optimization. *Mech. Struct. & Mach.*, **25**(4), 493–524.
Thompson, J. M. T. (1969). A general theory for the equilibrium and stability of discrete conservative systems. *ZAMP*, **20**, 797–846.